

DOI:10.16562/j.cnki.0256-1492.2017032001

# MIS3 以来天山黄土沉积速率时空分布规律及其意义

程良清<sup>1,2</sup>, 宋友桂<sup>1</sup>, 孙焕宇<sup>3</sup>, Rustam Orozbaev<sup>4</sup>

1. 中国科学院地球环境研究所黄土与第四纪地质国家重点实验室, 西安 710061

2. 中国科学院大学, 北京 100049

3. 福建师范大学地理科学学院, 福州 350007

4. Institute of Geology, National Academy of Sciences of Kyrgyz Republic, Bishkek 720040, Kyrgyzstan

**摘要:**风尘堆积沉积速率的变化对揭示大气环流与古气候变化具有重要意义。基于中亚东北部天山及其周边黄土剖面已有的释光和放射性<sup>14</sup>C年代数据的分析筛选整理,初步获得了该区深海氧同位素 MIS3 以来黄土沉积速率的时空变化特征,并探讨了可能的原因。结果表明:(1)末次盛冰期(LGM)沉积速率总体上表现出天山西部低、伊犁盆地高的特征。这种空间变化特征可能与地形、大气环流以及伊犁盆地黄土的近源堆积有关。(2)LGM 和 MIS3b 时期是 MIS3 阶段以来主要的粉尘沉积阶段。MIS3b 时期沉积速率最高,LGM 次之,而全新世沉积速率较低。MIS3b 时期高的沉积速率可能与大规模的冰川发育有关。在全新世期间,中全新世的沉积速率相对较高,可能与中全新世气候湿润、地表捕获粉尘的能力强有关。

**关键词:**沉积速率;全新世;LGM;MIS3b;天山黄土

中图分类号:P535 文献标识码:A

## Spatio-temporal distribution of dust sedimentation rate of Tianshan loess since MIS3 and its implications

CHENG Liangqing<sup>1,2</sup>, SONG Yougui<sup>1</sup>, SUN Huanyu<sup>3</sup>, Rustam Orozbaev<sup>4</sup>

1. State Key Laboratory of Loess and Quaternary Geology, Institute of Earth Environment, Chinese Academy of Sciences, Xi'an 710061, China

2. University of Chinese Academy of Sciences, Beijing 100049, China

3. College of Geographical Sciences, Fujian Normal University, Fuzhou 350007, China

4. Institute of Geology, National Academy of Sciences of Kyrgyz Republic, Bishkek 720040, Kyrgyzstan

**Abstract:** Eolian loess is an important archive for understanding Quaternary environmental changes. The sedimentation rate of loess, as an important proxy to environmental changes, is helpful to revealing atmospheric circulation and paleoenvironmental changes. With the application of various dating methods especially the high-accuracy Optically Stimulated Luminescence (OSL), sedimentation rate has been widely applied to the orbital-scale and millennial-scale paleoclimatic changes recently in the study of Chinese Loess Plateau (CLP). Central Asia is also one of the main distribution areas of world loess. This paper is specially devoted to the spatio-temporal distribution pattern of dust sedimentation rate of the Tianshan loess in order to provide a new horizon for understanding paleoclimatic patterns in Central Asia, where sedimentation rate has been poorly studied. Therefore, we collected the available geochronological data including OSL and <sup>14</sup>C of the last glacial loess sections from the Tianshan Mountains of Central Asia in this paper, analyzed the reliability of age data and discussed spatial and temporal distribution pattern of the sedimentation rate. The results suggest that: (1) During the Last Glacial Maximum (LGM), sedimentation rate is relatively low in the west of Tianshan, but high in the Ili Basin. This spatial pattern of distribution is closely related to geographic and atmospheric conditions as well as proximal accumulation. (2) LGM and MIS3b are the main dust deposition stages since MIS3. In the Tianshan area, the sedimentation rate of MIS3b is higher than that of LGM. Since the solar insolation in the MIS3b stage is higher than that in the LGM stage, the westerly will bring more moisture from the Atlantic Ocean, Caspian Sea and Mediterranean Sea. In the Tianshan area, moisture is believed the main factor affecting glaciers. In this regard, the scale of glacier in the wetter MIS3b period is larger than that in the LGM period, and the intensified abrasion of the glaciers will bring in more fine particulate matters. (3) Sedimentation rate is low in Holocene, and the

**资助项目:**国家重点研发计划全球变化专项“亚洲大陆风尘时空分布及其与全球变化的联系”(2016YFA0601902);国家自然科学基金项目“中亚干旱区黄土记录的末次冰期以来气候变化与驱动机制”(41572162);中国科学院国际合作局对外合作重点项目“中亚黄土与第四纪变化”(132B61KYS20160002)

**作者简介:**程良清(1990—),男,硕士,第四纪地质与古气候专业,E-mail:chenglq@ieecas.cn

**收稿日期:**2017-03-20; **改回日期:**2017-05-11. 文凤英编辑

variations in sedimentation rate are similar to the ‘westerly model’. We speculate that the amount of dust in the atmosphere is relatively low in Holocene. Dust is mainly deposited under wet climate since humidity is conducive to vegetation and helpful for dust to settle down. More moisture will result in higher sedimentation rate.

**Key words:** dust sedimentary rate; Holocene; the last glacial maximum; MIS3b; Tianshan loess

黄土作为全球古粉尘的良好记录,为全球气候变化历史研究提供了重要载体。沉积速率作为黄土中反映古气候环境变化的一个重要指标<sup>[1,2]</sup>,对重建大气环流强度和粉尘浓度具有重要意义。早期沉积速率主要是通过粒度等指标来反映<sup>[3-6]</sup>,集中于构造和轨道尺度上的研究<sup>[7,8]</sup>。后来,随着光释光(OSL)、加速器质谱(AMS)技术等高精度年代学方法的发展,学者们逐渐认识到粒度的变化不总是与沉积速率的变化直接对应<sup>[9-11]</sup>。基于高精度的年代序列,大量的学者将沉积速率用于黄土高原末次冰期以来千年尺度的气候变化研究中<sup>[12-15]</sup>,发现黄土高原西部(六盘山以西)沉积速率较黄土高原东部高,黄土高原西部MIS2阶段沉积速率比MIS3阶段要高,而黄土高原东部MIS2阶段沉积速率比MIS3阶段要低,并得出黄土高原东部沉积速率主要取决于地表捕获粉尘能力和湿沉降比例<sup>[13]</sup>。这与以前认为的东亚季风区粉尘沉积速率直接记录东亚冬季风强弱变化<sup>[1,16]</sup>是有差异的。近些年来,随着西部大开发和“一带一路”战略的实施,中亚黄土年代学和古气候研究成为热点,不同学者对中亚地区单个剖面<sup>[17-21]</sup>或某个区域<sup>[22,23]</sup>的粉尘沉积速率进行了初步的研究,这些为系统研究中亚地区的粉尘沉积速率时空变化提供了重要的数据基础。

本文通过收集整理已有黄土剖面的年代数据,重点研究末次冰期深海氧同位素3阶段(MIS3,约57ka)以来的中亚天山地区粉尘沉积速率的时空变化特征,这对深入理解中亚末次冰期以来的古粉尘循环和古气候环境变化具有重要意义。

## 1 研究区概况

中亚以干旱和半干旱大陆性气候为主,主要受中纬度西风环流、北冰洋极锋以及西伯利亚高压控制<sup>[24]</sup>(图1)。降水受地理位置和地形影响较大<sup>[25]</sup>,其中伊犁盆地的降水量最高,年降水量可达800~1000 mm<sup>[26]</sup>,其次为天山北坡,年降水量为270mm<sup>[27]</sup>,天山东部和南部则分别由于天山和帕米尔高原的阻挡,年平均降水量仅为150mm<sup>[28]</sup>和12mm<sup>[29]</sup>。中亚地区高空盛行西风,地面风向则受局域地形的影响较大,伊犁盆地地面风以东风频率

最高,但是大风主要以西和偏西风为主<sup>[30]</sup>,天山北坡在西风环流和西伯利亚高压的强烈影响下,地面风主要以北风和西北风为主<sup>[31]</sup>。哈萨克斯坦和吉尔吉斯斯坦受北冰洋极锋和西风环流的影响较大,地面风以西北风为主。地面风大风时常伴随着尘暴活动的发生<sup>[30]</sup>,尘暴活动在粉尘的搬运过程中起着重要作用,如在天山地区,向西气流携带着尘暴活动扬起的粉尘向东搬运,遇到高山的阻挡能够迅速堆积下来<sup>[32]</sup>,中亚地区最老的风尘堆积可追溯到24Ma<sup>[33]</sup>,其主要分布于中亚山区的迎风坡<sup>[22]</sup>以及河流阶地<sup>[34]</sup>,集中于塔吉克斯坦的东南部瓦赫什谷地和帕米尔高原的西麓<sup>[32]</sup>,乌兹别克斯坦东部塔什干-费尔干纳盆地<sup>[35]</sup>,哈萨克斯坦东南部阿拉木图<sup>[36]</sup>-外伊犁阿拉套山、东北部平原和阿尔泰山麓地带以及中国新疆、天山山麓、昆仑山和塔城盆地<sup>[34,37]</sup>。已有研究表明,天山北坡黄土主要来自古尔班通古特沙漠(图1)<sup>[31,38]</sup>,而伊犁盆地以及西天山北坡的黄土主要来自以西的克孜库勒姆沙漠、莫因库姆沙漠、萨雷耶西科阿特劳沙漠<sup>[31,36]</sup>以及近源的河流沉积物<sup>[39-41]</sup>。

## 2 材料与方法

近几十年来,加速器质谱(AMS)<sup>14</sup>C、热释光(TL)和光释光(OSL)等测年方法被广泛用于黄土年龄的测定,然而不同测年方法所测得年龄存在较大差异。TL信号普遍难以晒退,尤其是对于年轻黄土信号残留量大<sup>[42,43]</sup>,目前TL测年很少用,而OSL测年和AMS<sup>14</sup>C则在黄土测年当中应用比较多。但是研究发现AMS<sup>14</sup>C年龄与OSL年龄之间存在较大差异<sup>[44,45]</sup>。最近的研究表明,大约25cal.kaBP以来,AMS<sup>14</sup>C和OSL年龄大体上能够保持一致性,但是对老于25cal.kaBP的有机质碳年代常常偏年轻<sup>[20,46]</sup>。一般认为AMS<sup>14</sup>C年龄的这种偏低主要是由于年轻碳污染造成的<sup>[44,47]</sup>。大量的学者使用不同粒径的石英用于中亚黄土光释光测年,比如,细颗粒(4~11μm)<sup>[17,28,36,44,45]</sup>,中颗粒(38~63μm)<sup>[19,20,23,47,48]</sup>,粗颗粒(63~90μm)<sup>[19,49]</sup>,90~250μm<sup>[18]</sup>。其中Lai<sup>[50]</sup>认为中颗粒(38~63μm)

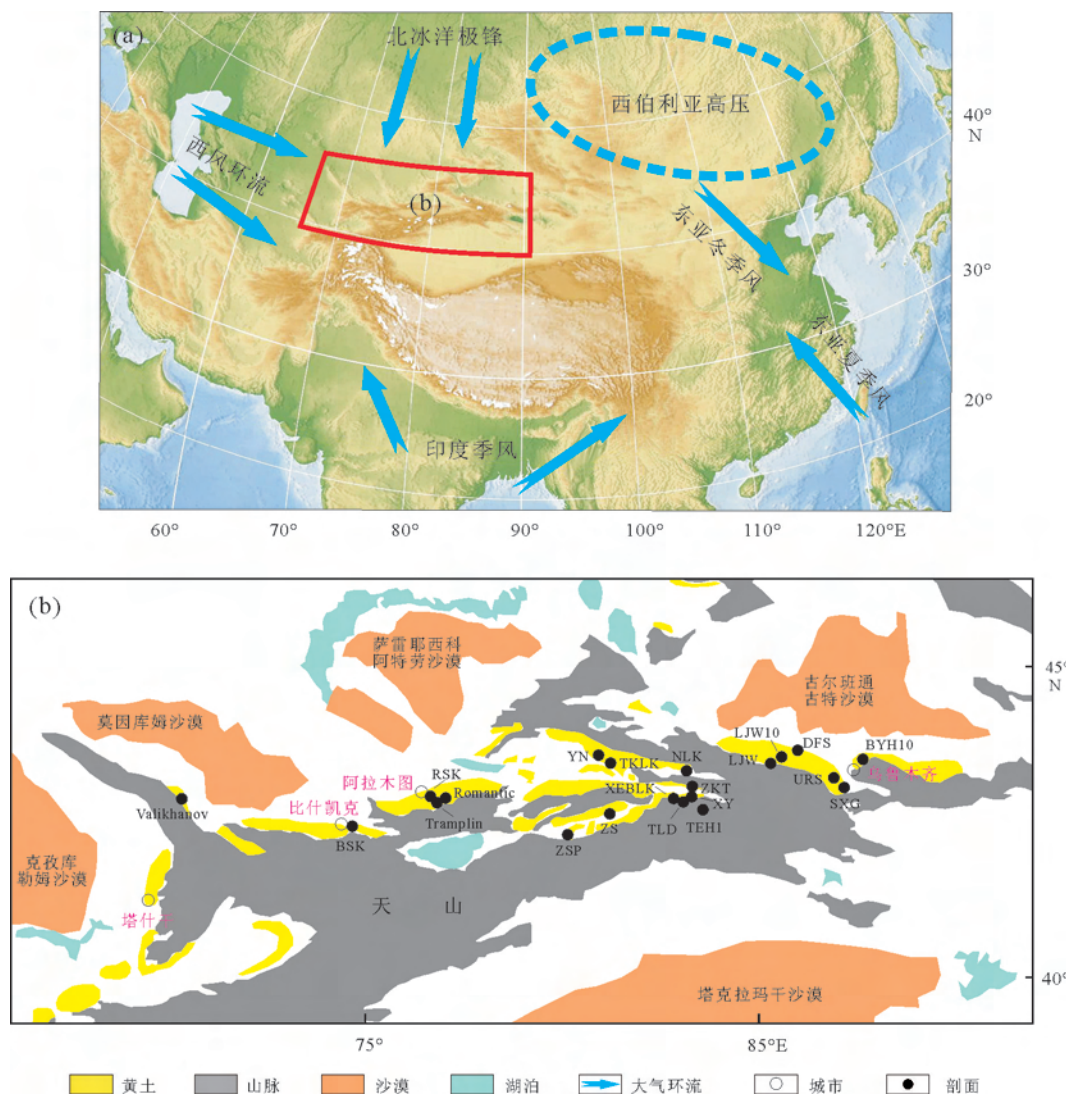


图1 亚洲大气环流特征(a)和天山黄土分布及剖面位置图(b)

Fig.1 Atmospheric circulation in Asia (a) and loess distribution in Tianshan area and locations of loess sections (b)

石英是较为理想的光释光测年材料,细颗粒在沉积之后有可能会发生淋溶、迁移和成土等过程,导致细颗粒组分的年代不能代表最后一次曝光事件,其次细颗粒很难去除没有释光信号的黏土矿物<sup>[51]</sup>。黄土中粗颗粒含量较少,很难提取到所要求的粗颗粒石英的量,另外粗颗粒提取过程中大量使用氢氟酸,氢氟酸对石英的溶蚀并不均匀(主要沿解理面进行溶蚀)<sup>[52]</sup>。也有学者提出粗颗粒较中颗粒和细颗粒要好,因为中颗粒和细颗粒必须计算 alpha 辐照剂量及剂量率,而粗颗粒石英可以避免 alpha 剂量率的计算,并且细颗粒和中颗粒可能存在不完全曝光问题,所测的年龄偏老<sup>[53]</sup>。然而,天山地区的黄土由于含有较多的近源堆积组分,可能导致石英尤其是粗颗粒石英释光信号灵敏度很低,不同粒径石英 OSL 测年结果不一致,具有一定复杂性。最近,康

树刚等<sup>[42]</sup>通过总结大量的文献认为,黄土在沉积前经过长时间的曝光,不同粒径的石英均能获得可靠的 OSL 年龄。AMS<sup>14</sup>C 的测年范围为 5 万年以内,石英 OSL 的测年范围为 8 万年以内,长石的灵敏度高,可以用来测试石英灵敏度低而无法得出可靠年代的样品,其测年范围比石英更广,如最新发展起来的钾长石的两步法(pIRIR)和多步法(MET-pIRIR)可达 30~40 万年<sup>[54]</sup>,是一个很有潜力的测年手段<sup>[42]</sup>。近些年,也有学者将钾长石 pIRIR 和 MET-pIRIR 方法用于中亚黄土测年,如天鹅湖(TEH1)剖面<sup>[55]</sup>、鹿角湾(LJW)和水西沟(SXG)剖面<sup>[27]</sup>、鹿角湾(LJW10)剖面<sup>[19]</sup>、白杨河(BYH10)剖面<sup>[22]</sup>。

虽说不同的测年手段所测得的年龄存在着差异,但是年代变化总体趋势类似,有一定的可比性。根据前人已发表的中亚东北部天山及周边的末次冰

期以来黄土剖面的年代数据(表1),参考前人研究黄土沉积速率的方法<sup>[22]</sup>,用Bacon年龄模型处理年代数据,计算平均沉积速率,分析影响沉积速率的因素(如离源区距离,源区的干旱程度,地形和大气环流,沉积区捕获粉尘的能力,沉积后的风蚀作用,年代的可靠程度等),探究中亚黄土沉积速率的时空变化规律。

### 3 结果与讨论

我们选择存在争议的4个剖面分析讨论年代的

可靠性(图2)。根据前人建立的新源县则克台镇附近的ZKT剖面的年代来看(图2a),ZKT剖面的OSL(SAR)<sup>[47]</sup>和OSL(SMAR)<sup>[45]</sup>年代之间保持了较好的一致性,而AMS<sup>14</sup>C的年代则明显低于OSL的年代(图2)。Feng等<sup>[45]</sup>认为ZKT剖面黄土主要来自河道扬起的粉尘近源堆积,从而导致曝光不充分,使得OSL的年代偏老。已有研究表明末次冰期近地面大风风向可能主要以西北风为主<sup>[41]</sup>,而ZKT剖面位于巩乃斯河北岸,因此很难想象会有大量扬起的河流沉积物在ZKT剖面沉积。AMS<sup>14</sup>C年代偏年轻则可能是由于用于AMS<sup>14</sup>C测年的蜗

表1 剖面位置、年代和厚度  
Table 1 Locations, ages and thickness

地点	剖面	经纬度坐标及海拔	厚度/m	剖面底部年龄/ka	测年材料及方法	文献来源
TLD1		43°25'N, 83°03'E	(12)	62.5	AMS <sup>14</sup> C 有机质	[30]
TLD2		43°24'5"N, 83°2'13"E; 1020m	100(5.1)	29	石英(4~11μm)SAR	[17]
TLD3		43°25'N, 83°03'E;	(33.5)	55	TL	[56]
ZKT1		43°31'53"N, 83°18'58"E; 850m	18	62.7	OSL	[25]
ZKT2		43°32'14"N, 83°18'50"E; 900m	23	72	石英(38~63μm)SAR	[47]
ZKT3		43°32'25"N, 83°18'10"E	22.5	46.7	AMS <sup>14</sup> C 蜗牛和 OSL	[45]
伊犁盆地	XY	43°27'N, 83°18'E;	(7)	41.4	TL	[25]
	ZSP	42°41'24"N, 80°15'00"E; 1875m	6.5	67	AMS <sup>14</sup> C 和石英(4~11μm)Post-IR	[44]
	ZS	43°08'99"N, 81°05'65"E; 1920m	4.5	56.9	AMS <sup>14</sup> C 沉积物	[25]
	XEblk	43°25'12"N, 83°04'12"E; 1050m	30.7	29	石英(38~63μm)SAR	[23]
	NLK1	43°45'36"N, 83°15'00"E; 1253m	21	69	石英(38~63μm)SAR	[20]
	NLK2	43°45'36"N, 83°15'00"E; 1253m	21	35.8	石英(63~90μm)SAR	[49]
	YN	44°00'N, 82°00'E;	(6)	9.4	TL	[56]
	TEH1	42°56'N, 84°E; 2400m	3.05	8.5	钾长石(150~200μm)pIRIR	[55]
	TKLK	43°52'06"N, 81°24'8"E; 636m	(5)	9.4	AMS <sup>14</sup> C 有机质	[56]
天山北坡	LJW	43°50'23"N, 85°07'35"E; 3641m	5(1.1)	7.1	钾长石(63~90μm)MET-pIRIR	[27]
	SXG	43°26'46"N, 87°30'27"E; 1636m	2(1.2)	8.7	钾长石(63~90μm)MET-pIRIR	[27]
	LJW10	43°58'29"N, 85°20'10"E; 1462m	2.8	12.6	钾长石(38~63μm)pIRIR	[19]
	DFS	玛纳斯河洪积扇台地, 527m	1.8	7	石英(40~63μm)BLSL	[48]
	BYH10	44°02'27"N, 87°47'54"E; 622m	30	71	钾长石(63~90μm)pIRIR	[22]
	URS	43°30'50"N, 87°19'48"E; 1603m	9.4	27.4	石英(4~11μm)SMAR	[28]
哈萨克斯坦 和吉尔吉斯斯坦	RSK1	43°13'N, 76°51'E; 1070m	80(40)	83	石英(4~11μm) IRSIL	[36]
	RSK2	43°13'N, 76°51'E; 1070m	80(8)	34.2	长石(4~11μm)PIR-IRSL	[21]
	Tramplin	43°12'31"N, 76°56'01"E; 1020m	10.5	40	AMS <sup>14</sup> C 蜗牛	[45]
	Romantic	43°12'31"N, 77°01'11"E; 1000m	9(5.9)	35	AMS <sup>14</sup> C 木炭、沉积物	[45]
	Valikhanov	43°10'30"N, 69°19'02"E; 1000m	7.5	25	AMS <sup>14</sup> C 沉积物	[45]
	BSK	42°42'15"N, 74°46'51"E; 1432m	30	60	石英(90~250μm)SAR	[18]

注:X(Y)表示总共X,其中上部Y作为研究对象。TLD-塔勒德,ZKT-则克台,XY-新源,ZSP-昭苏波马,ZS-昭苏,XEblk-肖尔布拉克,NLK-尼勒克,YN-伊宁,TEH-天鹅湖,TKLK-特克拉克,LJW-鹿角湾,SXG-水西沟,DFS-大佛寺,BYH-白杨河,URS-乌鲁木齐河剖面,RSK-Remizovka,BSK-比什凯克。

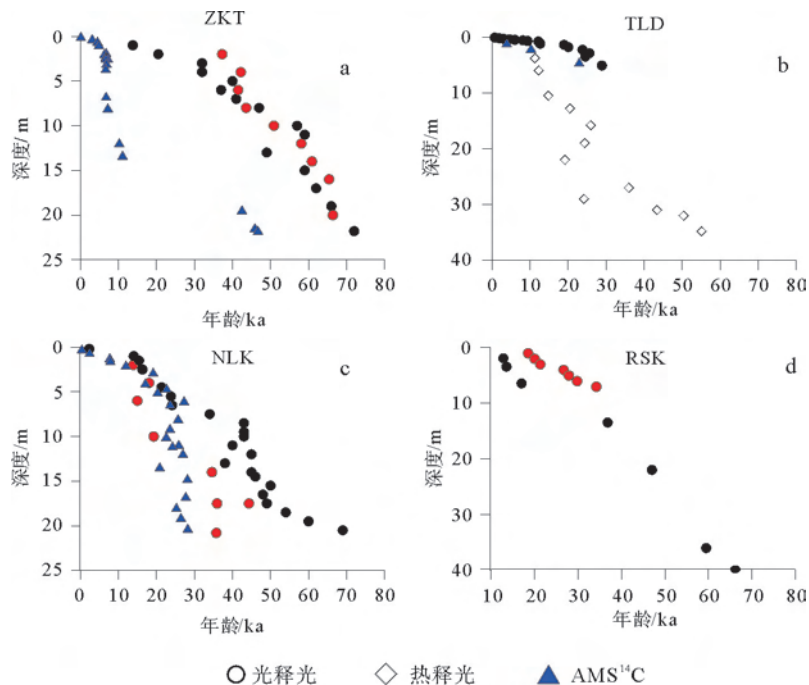


图2 ZKT、TLD、NLK、RSK剖面年代-深度图(数据来源见表1)  
(红圈和黑圈代表同一剖面不同方法的光释光年代结果)

Fig.2 Age and depth of ZKT, TLD, NLK, RSK sections(Data from Table 1)

牛,其在生长过程中可以在不同层位之间迁移,并且会受到年轻碳的影响<sup>[47]</sup>。

TLD剖面(图2b)的AMS<sup>14</sup>C<sup>[30]</sup>年龄和OSL<sup>[17]</sup>年龄比较接近,然而TL<sup>[56]</sup>年龄则与AMS<sup>14</sup>C和OSL年龄有较大差异,考虑到TL年代主要为20世纪90年代的测年结果,其精度和可靠性较差,因此,我们不采用TL的结果。NLK剖面(图2c)的中颗粒石英OSL<sup>[20]</sup>和粗颗粒石英OSL<sup>[49]</sup>也表现出较好的一致性,但是AMS<sup>14</sup>C年龄明显偏低<sup>[20]</sup>。从RSK剖面的年代来看(图2d),Machalett等<sup>[36]</sup>建立的细颗粒石英IRSL释光年代与Fitzsimmons等<sup>[21]</sup>建立的细颗粒长石pIR-IRSL释光年代之间则表现出较好的一致性。因此,根据年代的可靠性以及数据统计分析的要求,我们筛选出Valikhanov、BSK、XEBLK、NLK1、TLD2、ZKT2、RSK2、BYH10等8个剖面作出沉积速率变化图(图3)。

### 3.1 深海氧同位素 MIS3b

通过比较MIS3b时期(约44~54ka)<sup>[57]</sup>与LGM时期(约19~26ka)<sup>[58]</sup>的沉积速率发现(图3),除了BSK剖面可能存在沉积间断以外,NLK1、BYH10以及ZKT2剖面均表现出MIS3b时期沉积速率比LGM时期高。在风尘堆积年代学研究中,

年代分布频次在一定程度上可以反映期间沉积强度的变化<sup>[59]</sup>,这一理论已被成功应用于古气候变化研究中<sup>[60-64]</sup>。我们分析具有统计学意义的剖面年代分布情况也指示了MIS3b时期沉积强度较高(图4b)。古里雅冰芯记录MIS3b时期的温度低于现代5℃左右,呈现冰期气候特征<sup>[57]</sup>,并在全球多地区发现其冰川规模甚至比LGM时期要大<sup>[57]</sup>。最近天山周边的研究也表明MIS3b时期发育比LGM时期更大的冰川<sup>[65-68]</sup>,这促使MIS3b时期可能出现比LGM时期高的沉积速率。山地冰川发育,山体寒冻风化作用加强,形成较多的粉尘物质,寒冷且风力搬运能力增强,从而沉积速率高。

其次,BYH10剖面MIS3b时期沉积速率高达165cm/ka(图5),这可能与BYH10剖面所处的地理位置有关。BYH10剖面位于天山以东,受西伯利亚高压巨大冷源的强烈影响,加之天山的阻挡作用使得来自西边的水汽不容易达到天山以东。因此,天山以东地区冰阶气候较天山其他地区更加干冷,故而沉积速率较快。另外,沉积强度与65°N(7月)太阳辐射量曲线<sup>[70]</sup>表现出较好的对应关系,即在冰阶时,太阳辐射量低,气候干冷,源区大量的粉尘扬起,风沙活动频繁,沉积强度高;在间冰阶时,太阳辐射量高,气候暖湿,沉积强度低(图4c)。LGM

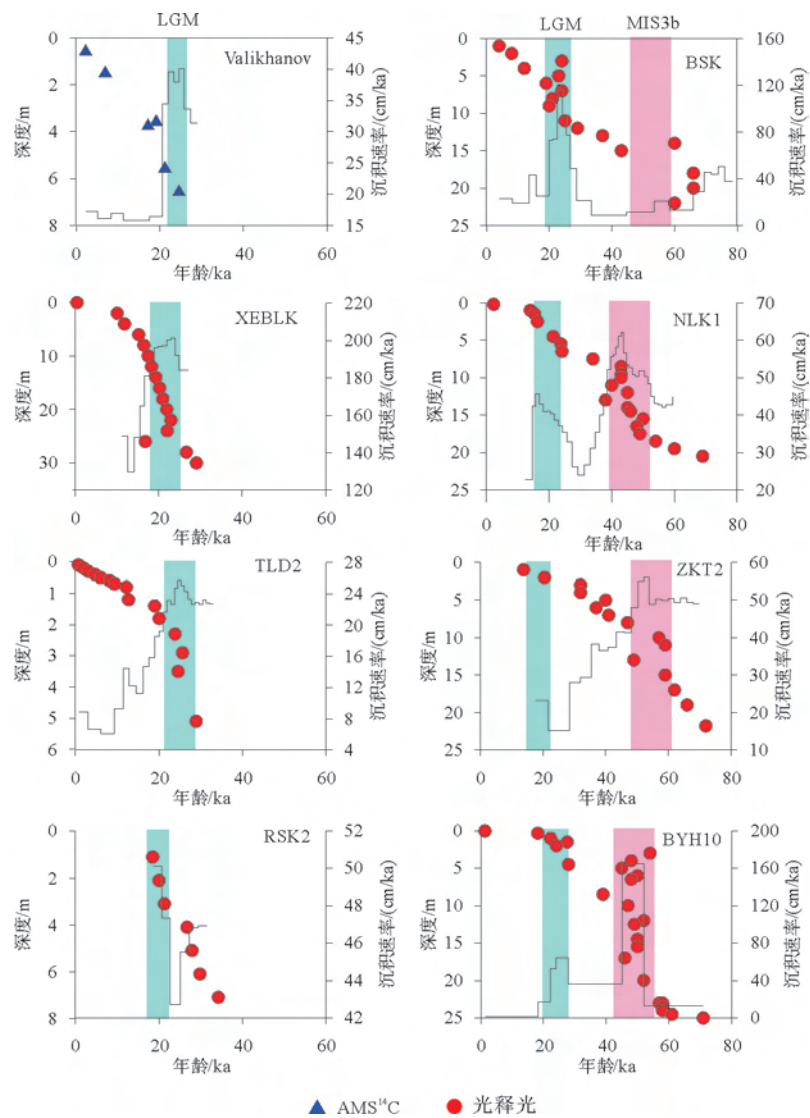


图3 MIS3以来天山黄土沉积速率变化(数据来源见表1)

Fig.3 Variations in sedimentation rate for Tian Shan loess since MIS3(Data from Table 1)

时期太阳辐射量低于 MIS3b,然而沉积强度却也比 MIS3b 时期要低,这可能与 MIS3b 时期天山地区冰量变化有关。已有学者提出在干旱的中亚地区,增加的冰量可能会使得西风带经向压缩,这种压缩效应同时会使得经向温度梯度增大,风力增强,风携带更多的粉尘物质,沉积强度大<sup>[21]</sup>。

### 3.2 末次冰盛期(LGM)

从图 3 可以看出,LGM 时期(19~26ka)<sup>[58]</sup>, Valikhanov、XEBLK、TLD2、RSK2、BSK、NLK1、ZKT2 以及 BYH10 剖面均表现出高值。年代分布情况(图 4b)同样也指示了 LGM 时期(19~26ka)沉积强度处于高值。古里雅冰芯(图 4a)在 15~26ka 之间含量较高的微粒浓度<sup>[69]</sup>说明了当时大气中粉尘浓度较高,同样也支持了我们的这一结论。伊犁

盆地为山间盆地,其沉积速率受地形影响较大(20~190cm/ka)<sup>[23]</sup>(图 5)。如位于伊犁盆地天山麓的剖面,由于高山的阻挡作用,大量的粉尘在山麓堆积,沉积速率较大(如 XEBLK、NLK);位于海拔较高的剖面(如 ZS:1920 m),由于粗颗粒粉尘难以被搬运至较高的海拔地区,只能沉积较小颗粒的粉尘,沉积速率低。伊犁盆地东西或南北向上没有表现出明显的变化趋势,但是平均沉积速率(TLD2、XEBLK、NLK1、ZS)为 70cm/ka,相对于西边哈萨克斯坦和吉尔吉斯斯坦黄土的平均沉积速率(Valikhanov、BSK、Romantic、RSK2)50cm/ka 要高。天山以东的 URS 剖面和 BYH10 剖面的沉积速率相差不大,平均沉积速率为 45cm/ka。大体上,中亚地区 LGM 时期从西部的哈萨克斯坦和吉尔吉斯斯坦到东部的伊犁盆地沉积速率增加,这也进一步证实了

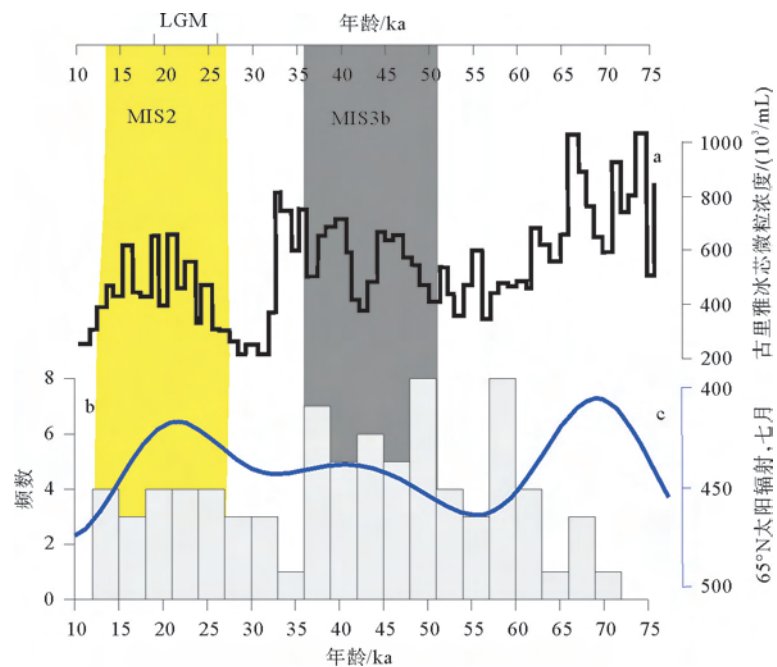


图4 古里雅冰芯微粒浓度<sup>[69]</sup>(a)、区域粉尘沉积年代频率(b)和65°N太阳辐射量<sup>[70]</sup>(c)对比  
Fig.4 Comparison of microparticle concentration of the Guliya ice core<sup>[69]</sup>(a), age frequency distribution of aeolian sedimentation (b), and insolation at 65°N<sup>[70]</sup>(c)

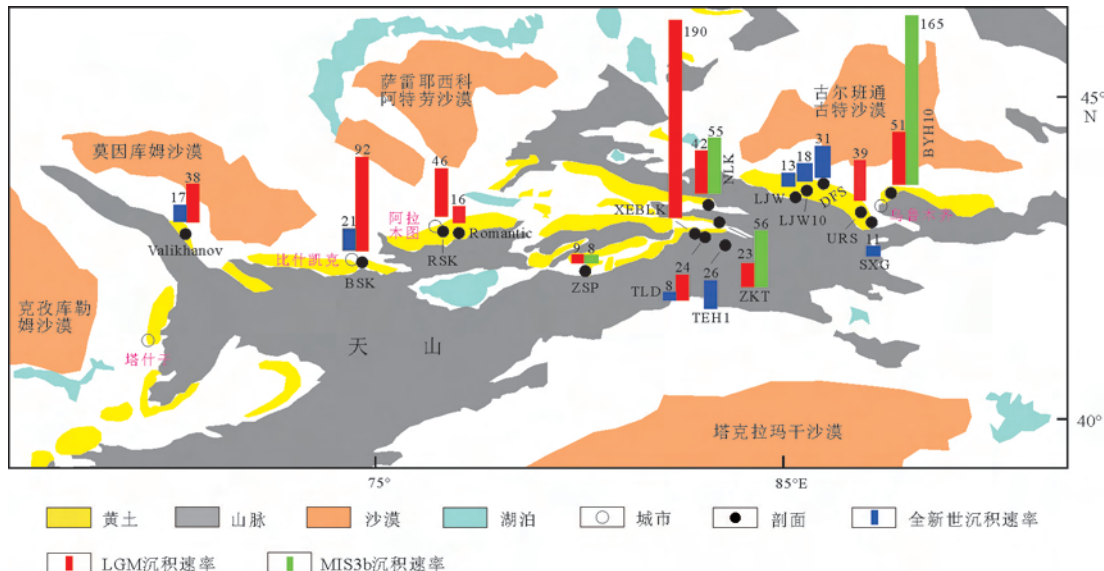


图5 中亚天山地区沉积速率空间变化  
Fig.5 Spatial variation in sedimentation rate in Central Asia

伊犁黄土含有大量的近源组分<sup>[39]</sup>。因为如果粉尘全部来自西边沙漠,那么离源区越远,沉积速率应越慢,换句话说就是东边伊犁盆地的沉积速率应该比西边的沉积速率要慢。LGM时期普遍较高的沉积速率可能与干冷的气候条件<sup>[70]</sup>和全球冰川扩张<sup>[71]</sup>有关。LGM时期天山山地冰川扩张<sup>[66-68]</sup>,对山体的寒冻风化作用加强,导致大量的粉尘物质产生,从而沉积速率也会增大<sup>[72,73]</sup>。

### 3.3 全新世

本文收集到10个天山及周边具有统计意义的新世黄土剖面,主要有TLD2、DFS、SXG、LJW、LJW10、TEH1、TKLK、ZKT3、XY、YN(表1)。其中TLD2、DFS用的是石英OSL测年方法,SXG、LJW、LJW10和TEH1剖面用的是钾长石pIRIR

测年方法,TKLK 和 ZKT3 剖面用的是 AMS<sup>14</sup>C 测年方法,XY、YN 用的是 TL 测年方法。考虑到 AMS<sup>14</sup>C 和 OSL 年龄在 25 cal.kaBP 之后能够表现出较好的一致性<sup>[20]</sup>,而 TL 用于年轻黄土的测年存在问题<sup>[42]</sup>,因此在分析过程中舍弃了 TL 年代。如前所述,ZKT3 剖面的 AMS<sup>14</sup>C 的年代可能存在着偏年轻的问题,因此我们采用了 TLD2、DFS、SXG、LJW、LJW10、TEH1、TKLK 等 7 个剖面的年代数据进行分析。全新世的沉积速率整体上比较低,大体上变化范围为 10~30cm/ka(图 5)。

我们根据全新世年代数据分析其年代频次的变化,考虑到年代的可靠性和年龄选取的无偏向性,我们没有选取出现明显倒转偏离的年龄和处于边界点的年龄(如 4ka 和 8ka)作为研究对象。统计结果显示,中全新世年代数据为 21 个,晚全新世 16 个,早全新世 11 个(图 6a)。说明全新世粉尘沉积强度在中全新世达到最大值,晚全新世次之,早全新世最小。Li 等<sup>[19]</sup>通过对天山北坡鹿角湾剖面(LJW10)全新世沉积速率的分析,也同样发现沉积速率在中全新世处于高值,晚全新世次之,早全新世最低。统计发现沉积强度的变化与西风区全新世湿度演化模式即“西风模式”<sup>[74]</sup>表现出较强的相似性(图 6b),“西风模式”认为中全新世(8~4ka)湿润,晚全新世(4~0ka)次之,早全新世(12~8ka)干旱。其他的研究也表明中亚地区早全新世干旱,中晚全新世湿润<sup>[27,55,62,75]</sup>。Yu 等<sup>[61]</sup>通过对柴达木盆地全新世剖

面年代分布频率的研究发现黄土年代数据主要集中在湿润的中全新世沉积,较湿润的晚全新世次之,而在干旱的早全新世最少。大量的研究证实沉积区地表捕获粉尘的能力对沉积速率是有影响的<sup>[10,76]</sup>。因此,我们推测天山地区全新世期间湿度越大,沉积速率越高。这与上文提到的干冷的 LGM 和 MIS3b 时期沉积速率高是有差异的。天山地区全新世期间,在没有足够多的粉尘扬起的情况下,湿沉降的比例会增加,其次,湿度越大,沉积区植被发育越好,沉积区地表捕获粉尘能力越强<sup>[76]</sup>。从而,全新世期间,湿度越大,粉尘的沉积强度越大和堆积速率越高。而较为干冷的 LGM 和 MIS3b 时期与源区粉尘的释放有很大关系,源区粉尘释放量大,沉积区沉积速率高<sup>[72,73]</sup>。当然,全新世时期湿度与沉积强度和沉积速率的关系还需要大量的工作进一步证实。

## 4 结论

(1)LGM 时期,沉积速率表现出天山西部低、中间伊犁盆地高的特征。这种变化特征可能与地形、大气环流和近源堆积密切相关。

(2)LGM 和 MIS3b 时期是 MIS3 阶段以来主要的粉尘沉积阶段,MIS3b 时期粉尘堆积速率最高,LGM 时期次之,全新世粉尘堆积速率最低。MIS3b 时期的高沉积速率可能与大规模的冰川发育有关,在全新世期间,中全新世的沉积速率相对高,可能与中全新世气候湿润,地表捕获粉尘的能力强有关。

## 参考文献(References)

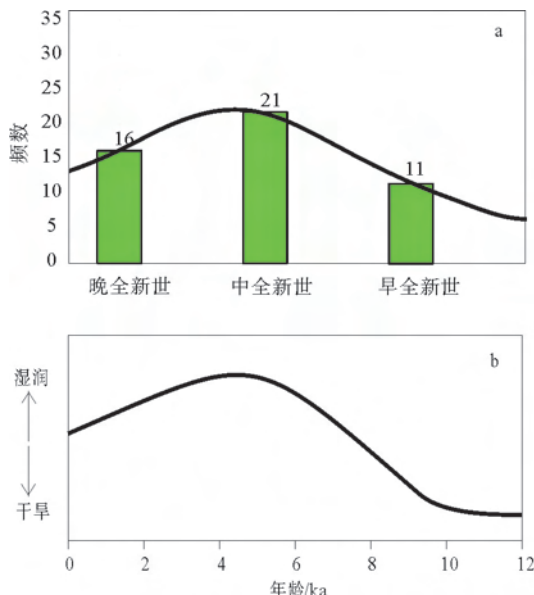


图 6 天山全新世黄土年代分布频数特征(a)  
及其与西风模式对比(b)(据 Chen 等<sup>[74]</sup>)

Fig.6 Age frequency distribution of Holocene Tianshan loess  
(a) and westerly climate model (b) in Central Asia<sup>[74]</sup>

- [1] Pye K. The nature, origin and accumulation of loess[J]. Quaternary Science Reviews, 1995, 14: 653-667.
- [2] Roberts H M. The Development and Application of Luminescence Dating to Loess Deposits: a Perspective on the Past, Present and Future[J]. Boreas, 2008, 37: 484-507.
- [3] Porter S C, An Z. Correlation between climate events in the North Atlantic and China during the last glaciation[J]. Nature, 1995, 375: 305-308.
- [4] 鹿化煜, 安芷生, Vandenberghe J, 等. 洛川黄土地层定年的一个模式及其初步应用[J]. 沉积学报, 1997, 15(3): 150-152.  
[LU Huayu, AN Zhisheng, Vandenberghe J, et al. A dating model of loess stratigraphy in the central Chinese Loess Plateau and its preliminary application [J]. Acta Sedimentologica Sinica, 1997, 15(3): 150-152.]
- [5] An Z S. The history and variability of the East Asian paleomonsoon climate[J]. Quaternary Science Reviews, 2000, 19:

- 171-187.
- [6] Kohfeld K. Glacial-interglacial changes in dust deposition on the Chinese Loess Plateau[J]. Quaternary Science Reviews, 2003, 22(18-19): 1859-1878.
- [7] Sun Y B, An Z S. Late Pliocene-Pleistocene changes in mass accumulation rates of eolian deposits on the central Chinese Loess Plateau[J]. Journal of Geophysical Research, 2005, 110: D23101.
- [8] Guo Z T, Ruddiman W F, Hao Q Z, et al. Onset of Asian desertification by 22 Myr ago inferred from loess deposits in China[J]. Nature, 2002, 416: 159-163.
- [9] Stevens T, Lu H, Thomas D S G, et al. Optical dating of abrupt shifts in the Late Pleistocene East Asian Monsoon[J]. Geology, 2008, 36(5): 415.
- [10] Lu Y C, Wang X L, Wintle A G. A new OSL chronology for dust accumulation in the last 130000 yr for the Chinese Loess Plateau[J]. Quaternary Research, 2007, 67(1): 152-160.
- [11] Lai Z P, Wintle A G, Thomas D S G. Rates of dust deposition between 50ka and 20ka revealed by OSL dating at Yuanbaotao on the Chinese Loess Plateau[J]. Palaeogeography, Palaeoclimatology, Palaeoecology, 2007, 248(3-4): 431-439.
- [12] Kang S G, Roberts H M, Wang X L, et al. Mass accumulation rate changes in Chinese loess during MIS 2, and asynchrony with records from Greenland ice cores and North Pacific Ocean sediments during the Last Glacial Maximum[J]. Aeolian Research, 2015, 19: 251-258.
- [13] Kang S G, Wang X L, Lu Y C. Quartz OSL chronology and dust accumulation rate changes since the Last Glacial at Weinan on the southeastern Chinese Loess Plateau[J]. Boreas, 2013, 42(4): 815-829.
- [14] Buylaert J P, Murray A S, Vandenberghe D, et al. Optical dating of Chinese loess using sand-sized quartz: Establishing a time frame for Late Pleistocene climate changes in the western part of the Chinese Loess Plateau[J]. Quaternary Geochronology, 2008, 3(1-2): 99-113.
- [15] Stevens T, Buylaert J-P, Lu H, et al. Mass accumulation rate and monsoon records from Xifeng, Chinese Loess Plateau, Based on a luminescence age model[J]. Journal of Quaternary Science, 2016, 31(4): 391-405.
- [16] 刘东生. 黄土与环境[M]. 北京: 科学出版社, 1985; 41-81.  
[LIU Tungsheng. Loess and Environment [M]. Science Press, Beijing, 1985; 44-81.]
- [17] Kang S G, Wang X L, Lu Y C, et al. A high-resolution quartz OSL chronology of the Talede loess over the past ~30ka and its implications for dust accumulation in the Ili Basin, Central Asia[J]. Quaternary Geochronology, 2015, 30: 181-187.
- [18] Youn J H, Seong Y B, Choi J H, et al. Loess deposits in the northern Kyrgyz Tien Shan: Implications for the paleoclimate reconstruction during the Late Quaternary[J]. Catena, 2014, 117: 81-93.
- [19] Li G Q, Wen L J, Xia D S, et al. Quartz OSL and K-feldspar pIRIR dating of a loess/paleosol sequence from arid central Asia, Tianshan Mountains, NW China[J]. Quaternary Geochronology, 2015, 28: 40-53.
- [20] Song Y G, Lai Z P, Li Y, et al. Comparison between luminescence and radiocarbon dating of late Quaternary loess from the Ili Basin in Central Asia[J]. Quaternary Geochronology, 2015, 30: 405-410.
- [21] Fitzsimmons K E, Sprafke T, Zielhofer C, et al. Loess accumulation in the Tian Shan piedmont: Implications for palaeoenvironmental change in arid Central Asia[J]. Quaternary International, 2018, 469: 30-43.
- [22] Li G Q, Rao Z G, Duan Y W, et al. Paleoenvironmental changes recorded in a luminescence dated loess/paleosol sequence from the Tianshan Mountains, arid central Asia, since the penultimate glaciation[J]. Earth and Planetary Science Letters, 2016, 448: 1-12.
- [23] Li Y, Song Y G, Lai Z P, et al. Rapid and cyclic dust accumulation during MIS 2 in central Asia inferred from loess OSL dating and grainsize analysis[J]. Scientific Reports, 2016, 6: 32365.
- [24] Dodonov A E, Baiguzina L L. Loess stratigraphy of central Asia: Paleoclimatic and Palaeoenvironmental aspects[J]. Quaternary Science Review, 1995, 95: 707-720.
- [25] 叶伟. 新疆西风区黄土沉积特征与古气候[M]. 北京: 海洋出版社, 2001. [YE Wei. Loess Deposition Features and Paleoclimate in the Westerlies-Dominated Region of Xinjiang [M]. Ocean Press, Beijing, 2001.]
- [26] Li X Q, Zhao K L, Dodson J, et al. Moisture dynamics in central Asia for the last 15 kyr: New evidence from Yili Valley, Xinjiang, NW China[J]. Quaternary Science Reviews, 2011, 30(23-24): 3457-3466.
- [27] Zhao H, Li S-H, Li B, et al. Holocene climate changes in westerly-dominated areas of central Asia: Evidence from optical dating of two loess sections in Tianshan Mountain, China[J]. Quaternary Geochronology, 2015, 30: 188-193.
- [28] Lu H H, Xu Y D, Niu Y, et al. Late Quaternary loess deposition in the southern Chaiwopu Basin of the northern Chinese Tian Shan foreland and its palaeoclimatic implications[J]. Boreas, 2016, 45(2): 304-321.
- [29] 潘燕芳. 昆仑山北坡全新世黄土记录的环境变化[D]. 乌鲁木齐: 中国科学院新疆生态与地理研究所, 2013. [PAN Yanfang. Holocene Loess Deposits and Environmental Changes on the Northern Slope of Kunlun Mountains, Xinjiang, China [D]. Xinjiang Institute of Ecology and Geography Chinese Academy of Sciences, Urumqi, 2013.]
- [30] 史正涛. 伊犁黄土形成时代及环境研究[D]. 西安: 中国科学院地球环境研究所, 2005. [SHI Zhengtao. Age of Yili Loess in Xinjiang and Its Paleoenvironmental Implications [D]. Institute of Earth Environment, Chinese Academy of Sciences, 2005.]
- [31] Sun J M. Source regions and formation of the loess sediments on the high mountain regions of northwestern China[J]. Quaternary Research, 2002, 58(3): 341-351.
- [32] Ding Z L, Ranov V, Yang S L, et al. The loess record in

- southern Tajikistan and correlation with Chinese loess [J]. Earth and Planetary Science Letters, 2002, 200: 387-400.
- [33] Sun J M, Ye J, Wu W Y, et al. Late Oligocene-Miocene mid-latitude aridification and wind patterns in the Asian interior [J]. Geology, 2010, 38(6): 515-518.
- [34] Song Y G, Chen X L, Qian L B, et al. Distribution and composition of loess sediments in the Ili Basin, Central Asia [J]. Quaternary International, 2014, 334-335: 61-73.
- [35] Mavlyanov G A, Academician P, Kasymov S M, et al. The Uzbekistan Loess, genesis and distribution [J]. GeoJournal, 1987, 15(2): 145-150.
- [36] Machalett B, Frechen M, Hambach U, et al. The loess sequence from Remisowka (northern boundary of the Tien Shan Mountains, Kazakhstan)—Part I: Luminescence dating [J]. Quaternary International, 2006, 152-153: 192-201.
- [37] Li Y, Song Y G, Yan L B, et al. Timing and spatial distribution of loess in Xinjiang, NW China [J]. Plos One, 2015, 10(5): e0125492.
- [38] Fang X M, Shi Z T, Yang S L, et al. Loess in the Tian Shan and its implications for the development of the Gurbantunggut Desert and drying of northern Xinjiang [J]. Chinese Science Bulletin, 2002, 47(6): 1381-1387.
- [39] 李传想, 宋友桂, 王乐民. 伊犁盆地黄土分布、年代及粉尘来源分析 [J]. 地球与环境, 2012, 40(3): 314-320. [LI Chuangxiang, SONG Yougui, WANG Lemin. Distribution, age and dust sources of loess in the Ili Basin [J]. Earth And Environment, 2012, 40(3): 314-320.]
- [40] 叶玮, 靳鹤龄, 赵兴有等. 新疆伊犁地区黄土的粒度特征与物质来源 [J]. 干旱区地理, 1998, 21(4): 1-8. [YE Wei, JIN Heling, ZHAO Xingyou, et al. Depositional features and material sources of loess in Yili region, Xinjiang [J]. Arid Land Geography, 1998, 21(4): 1-8.]
- [41] 史正涛, 董铭. 天山黄土粒度特征及粉尘来源 [J]. 云南师范大学学报, 2007, 27(3): 55-58. [SHI Zhengtao, DONG Ming. Characteristics of loess grain size and source of dust in Tianshan, China [J]. Journal of Yunnan Normal University, 2007, 27(3): 55-58.]
- [42] 康树刚, 王旭龙, 王松娜. 中国黄土释光测年与应用:过去、现在与未来 [J]. 地球环境学报, 2016, 7(5): 442-467. [KANG Shugang, WANG Xulong, WANG Songna. Luminescence dating of Chinese Loess and its applications: past, present and future [J]. Journal of Earth Environment, 2016, 7(5): 442-467.]
- [43] Lu Y C, Zhang J Z, Xie J. Thermoluminescence dating of loess and palaeosols from the Lantian section, Shaanxi Province, China [J]. Quaternary Science Reviews, 1988, 7: 245-250.
- [44] Song Y G, Li C X, Zhao J D, et al. A combined luminescence and radiocarbon dating study of the Ili loess, central Asia [J]. Quaternary Geochronology, 2012, 10: 2-7.
- [45] Feng Z D, Ran M, Yang Q L, et al. Stratigraphies and chronologies of late Quaternary loess-paleosol sequences in the core area of the central Asian arid zone [J]. Quaternary International, 2011, 240(1-2): 156-166.
- [46] Long H, Shen J, Wang Y, et al. High-resolution OSL dating of a late Quaternary sequence from Xingkai Lake (NE Asia): Chronological challenge of the “MIS 3a Mega-paleolake” hypothesis in China [J]. Earth and Planetary Science Letters, 2015, 428: 281-292.
- [47] E C Y, Lai Z P, Sun Y J, et al. A luminescence dating study of loess deposits from the Yili River basin in western China [J]. Quaternary Geochronology, 2012, 10: 50-55.
- [48] 葛本伟, 刘安娜. 天山北麓黄土沉积的光释光年代学及环境敏感粒度组分研究 [J]. 干旱区资源与环境, 2017, 31(2): 110-116. [GE Benwei, LIU Anna. Optically stimulated luminescence dating and analysis of environmentally sensitive grain-size component of loess in the northern slope of Tian Shan [J]. Journal of Arid Land Resources and Environment, 2017, 31(2): 110-116.]
- [49] Yang S L, Forman S L, Song Y G, et al. Evaluating OSL-SAR protocols for dating quartz grains from the loess in Ili Basin, central Asia [J]. Quaternary Geochronology, 2014, 20: 78-88.
- [50] Lai Z P. Chronology and the upper dating limit for loess samples from Luochuan section in the Chinese Loess Plateau using quartz OSL SAR protocol [J]. Journal of Asian Earth Sciences, 2010, 37(2): 176-185.
- [51] Krabetschek M R, Götze J, Dietrich A, et al. Spectral information from minerals relevant for luminescence dating [J]. Radiation Measurements, 1997, 27: 695-748.
- [52] 赖忠平, 欧先交. 光释光测年基本流程 [J]. 地理科学进展, 2013, 32(5): 683-693. [LAI Zhongping, OU Xianjiao. Basic procedures of optically stimulated luminescence (OSL) dating [J]. Process in Geography, 2013, 32(5): 683-693.]
- [53] Yang H, Chen J, Thompson J A, et al. Optical dating of the 12 May 2008, Ms 8.0 Wenchuan earthquake-related sediments: Tests of zeroing assumptions [J]. Quaternary Geochronology, 2012, 10: 273-279.
- [54] Buylaert J-P, Jain M, Murray A S, et al. A robust feldspar luminescence dating method for Middle and Late Pleistocene sediments [J]. Boreas, 2012, 41(3): 435-451.
- [55] Long H, Shen J, Tsukamoto S, et al. Dry early Holocene revealed by sand dune accumulation chronology in Bayanbulak Basin (Xinjiang, NW China) [J]. The Holocene, 2014, 24(5): 614-626.
- [56] 史正涛. 天山黄土与西北内陆干旱化 [D]. 兰州: 兰州大学, 2002. [SHI Zhengtao. Mountains and Its Implication of Drying and Desertification in Xinjiang, Northwest China [D]. Lanzhou University, 2002.]
- [57] 施雅风. 中国第四纪冰期划分改进建议 [J]. 冰川冻土, 2002, 24(6): 687-692. [SHI Yafeng. A suggestion to improve the chronology of Quaternary glaciations in China [J]. Journal of Glaciology and Geocryology, 2002, 24(6): 687-692.]
- [58] Clark P U, Dyke A S, Shakun J D, et al. The Last Glacial Maximum [J]. Science, 2009, 325: 710-715.
- [59] Singhvi A K, Bluszcz A, Bateman M D, et al. Luminescence

- dating of loess-palaeosol sequences and coversands: methodological aspects and palaeoclimatic implications[J]. *Earth-Science Reviews*, 2001, 54: 193-211.
- [60] Qiang M R, Chen F H, Song L, et al. Late Quaternary aeolian activity in Gonghe Basin, northeastern Qinghai-Tibetan Plateau, China[J]. *Quaternary Research*, 2013, 79(3): 403-412.
- [61] Yu L P, Lai Z P. OSL chronology and palaeoclimatic implications of aeolian sediments in the eastern Qaidam Basin of the northeastern Qinghai-Tibetan Plateau[J]. *Palaeogeography, Palaeoclimatology, Palaeoecology*, 2012, 337-338: 120-129.
- [62] Chen F H, Wu D, Chen J H, et al. Holocene moisture and East Asian summer monsoon evolution in the northeastern Tibetan Plateau recorded by Lake Qinghai and its environs: A review of conflicting proxies[J]. *Quaternary Science Reviews*, 2016, 154: 111-129.
- [63] Stauch G, Lai Z P, Lehmkühl F, et al. Environmental changes during the late Pleistocene and the Holocene in the Gonghe Basin, north-eastern Tibetan Plateau[J]. *Palaeogeography, Palaeoclimatology, Palaeoecology*, 2018, 509: 144-155.
- [64] Wang X, Yi S, Lu H, et al. Aeolian process and climatic changes in loess records from the northeastern Tibetan Plateau: Response to global temperature forcing since 30ka[J]. *Paleoceanography*, 2015, 30(6): 612-620.
- [65] Lifton N, Beel C, Hättestrand C, et al. Constraints on the late Quaternary glacial history of the Inylchek and Sary-Dzaz valleys from in situ cosmogenic  $^{10}\text{Be}$  and  $^{26}\text{Al}$ , eastern Kyrgyz Tian Shan[J]. *Quaternary Science Reviews*, 2014, 101: 77-90.
- [66] Zhao J D, Liu S Y, Wang J, et al. Glacial advances and ESR chronology of the Pochengzi Glaciation, Tianshan Mountains, China[J]. *Science China Earth Sciences*, 2009, 53(3): 403-410.
- [67] Zhao J D, Song Y G, King J W, et al. Glacial geomorphology and glacial history of the Muzart River valley, Tianshan Range, China[J]. *Quaternary Science Reviews*, 2010, 29(11-12): 1453-1463.
- [68] Zhao J D, Yin X F, Harbor J M, et al. Quaternary glacial chronology of the Kanas River valley, Altai Mountains, China[J]. *Quaternary International*, 2013, 311: 44-53.
- [69] Wu G J. Microparticle record in the Guliya ice core and its comparison with polar records since the Last Interglacial[J]. *Chinese Science Bulletin*, 2004, 49(6): 607-611.
- [70] Cheng H, Zhang P Z, Spötl C, et al. The climatic cyclicity in semiarid-arid central Asia over the past 500000 years[J]. *Geophysical Research Letters*, 2012, 39(1): L01705.
- [71] Narama C, Kondo R, Tsukamoto S, et al. OSL dating of glacial deposits during the Last Glacial in the Terskey-Alatau Range, Kyrgyz Republic[J]. *Quaternary Geochronology*, 2007, 2(1-4): 249-254.
- [72] Mahowald N, Kohfeld K, Hansson M, et al. Dust sources and deposition during the last glacial maximum and current climate: A comparison of model results with paleodata from ice cores and marine sediments[J]. *Journal of Geophysical Research: Atmospheres*, 1999, 104(D13): 15895-15916.
- [73] Reader M C, Fung I, McFarlane N. Mineral aerosols: a comparison of the last glacial maximum and preindustrial Holocene[J]. *Canadian Journal of Earth Sciences*, 2000, 37: 751-767.
- [74] Chen F H, Yu Z C, Yang M l, et al. Holocene moisture evolution in arid central Asia and its out-of-phase relationship with Asian monsoon history [J]. *Quaternary Science Reviews*, 2008, 27(3-4): 351-364.
- [75] An C B, Lu Y B, Zhao J J, et al. A high-resolution record of Holocene environmental and climatic changes from Lake Balikun (Xinjiang, China): Implications for central Asia[J]. *The Holocene*, 2011, 22(1): 43-52.
- [76] Küster Y, Hetzel R, Krötschek M, et al. Holocene loess sedimentation along the Qilian Shan (China): significance for understanding the processes and timing of loess deposition [J]. *Quaternary Science Reviews*, 2006, 25(1-2): 114-125.